

University of Groningen

Efficient Conversions of Macroalgae-Derived Anhydrosugars to 5-Hydroxymethylfurfural and Levulinic Acid

Martina, Angela; Stojkov, Gorjan; van de Bovenkamp, Henk H.; Wang, Ting; Deuss, Peter J.; Noordergraaf, Inge W.; Winkelman, Jozef G.M.; Picchioni, Francesco; Heeres, Hero J.

Published in:
Industrial and Engineering Chemistry Research

DOI:
[10.1021/acs.iecr.3c01357](https://doi.org/10.1021/acs.iecr.3c01357)

IMPORTANT NOTE: You are advised to consult the publisher's version (publisher's PDF) if you wish to cite from it. Please check the document version below.

Document Version
Publisher's PDF, also known as Version of record

Publication date:
2023

[Link to publication in University of Groningen/UMCG research database](#)

Citation for published version (APA):

Martina, A., Stojkov, G., van de Bovenkamp, H. H., Wang, T., Deuss, P. J., Noordergraaf, I. W., Winkelman, J. G. M., Picchioni, F., & Heeres, H. J. (2023). Efficient Conversions of Macroalgae-Derived Anhydrosugars to 5-Hydroxymethylfurfural and Levulinic Acid: The Remarkable Case of 3,6-Anhydro-d-galactose. *Industrial and Engineering Chemistry Research*, 62(39), 15821-15833. <https://doi.org/10.1021/acs.iecr.3c01357>

Copyright

Other than for strictly personal use, it is not permitted to download or to forward/distribute the text or part of it without the consent of the author(s) and/or copyright holder(s), unless the work is under an open content license (like Creative Commons).

The publication may also be distributed here under the terms of Article 25fa of the Dutch Copyright Act, indicated by the "Taverne" license. More information can be found on the University of Groningen website: <https://www.rug.nl/library/open-access/self-archiving-pure/taverne-amendment>.

Take-down policy

If you believe that this document breaches copyright please contact us providing details, and we will remove access to the work immediately and investigate your claim.

Downloaded from the University of Groningen/UMCG research database (Pure): <http://www.rug.nl/research/portal>. For technical reasons the number of authors shown on this cover page is limited to 10 maximum.

Efficient Conversions of Macroalgae-Derived Anhydrosugars to 5-Hydroxymethylfurfural and Levulinic Acid: The Remarkable Case of 3,6-Anhydro-D-galactose

Published as part of the *Industrial & Engineering Chemistry Research virtual special issue "Dmitry Murzin Festschrift"*.

Angela Martina, Gorjan Stojkov, Henk H. van de Bovenkamp, Ting Wang, Peter J. Deuss, Inge W. Noordergraaf, Jozef G. M. Winkelman, Francesco Picchioni, and Hero J. Heeres*

Cite This: *Ind. Eng. Chem. Res.* 2023, 62, 15821–15833

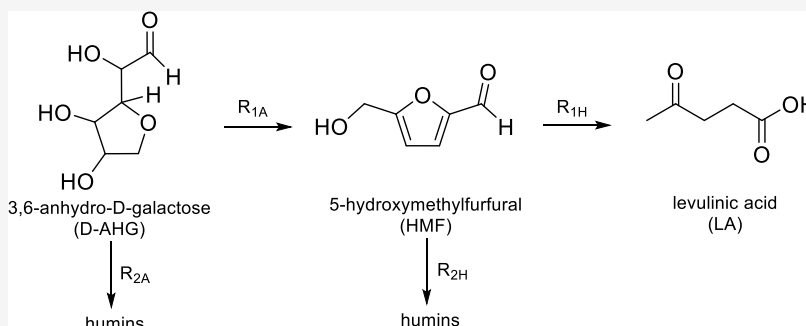
Read Online

ACCESS |

Metrics & More

Article Recommendations

Supporting Information



ABSTRACT: Macroalgae or seaweed is considered a renewable and sustainable resource to produce biobased fuels, polymers, and chemicals due to its high content of polysaccharides. Various studies have reported the obtained 5-hydroxymethylfurfural (HMF) and levulinic acid (LA) from seaweeds. However, the source of the saccharides that is responsible for HMF formation, accurate yield data (often only HMF concentrations are given instead of yields on feed), and the reaction pathways (including byproducts) is not well understood. We here report a kinetic study on the conversion of 3,6-anhydro-D-galactose (D-AHG), one of the main building blocks of the polysaccharides in seaweed, to HMF and LA in water using sulfuric acid as a catalyst with the aim to rationalize and optimize the production of HMF and LA from seaweeds. The experiments were carried out in batch at temperatures between 160 and 200 °C using various initial concentrations of D-AHG (0.006–0.06 M) and sulfuric acid (0.0025–0.05 M) as the catalyst. The highest experimental yield of HMF within this range of experimental conditions was remarkably high (61 mol %) and obtained at 160 °C, with a low initial D-AHG concentration (0.006 M) and a low acid concentration (0.0025 M). These findings imply that D-AHG is a very good precursor for the HMF synthesis. Additional experiments outside the experimental window gave an even higher HMF yield of 67 mol %. The highest LA yields were 51 mol % [160 °C, low initial D-AHG concentration (0.006 M), and high acid concentration (0.05 M)]. The experimental data were modeled using a power law approach, and the kinetic model was used to determine reactor configurations giving the maximum yield of HMF and LA. The result showed that a plug flow reactor is favorable to achieve the highest yield of HMF, whereas a continuously ideally stirred tank reactor is the preferable reactor configuration to obtain the highest yield of LA.

1. INTRODUCTION

Biomass is an interesting renewable resource to produce fuels and chemicals. Examples of interesting platform chemicals with a broad application potential are 5-hydroxymethylfurfural (HMF) and levulinic acid (LA).¹ HMF may be converted to polymer building blocks like 2,5-furandicarboxylic acid, 5-hydroxymethylfuroic acid, adipic acid, and caprolactone.² Also, LA is considered a multipurpose building block for, among others solvents, fuel additives, plasticizers, and polymer precursors.³

In recent years, macroalgae or seaweeds have received considerable attention and particularly to serve as a marine biomass source for the synthesis of biobased chemicals.^{4,5} They

Received: April 24, 2023

Revised: August 31, 2023

Accepted: August 31, 2023

Published: September 22, 2023



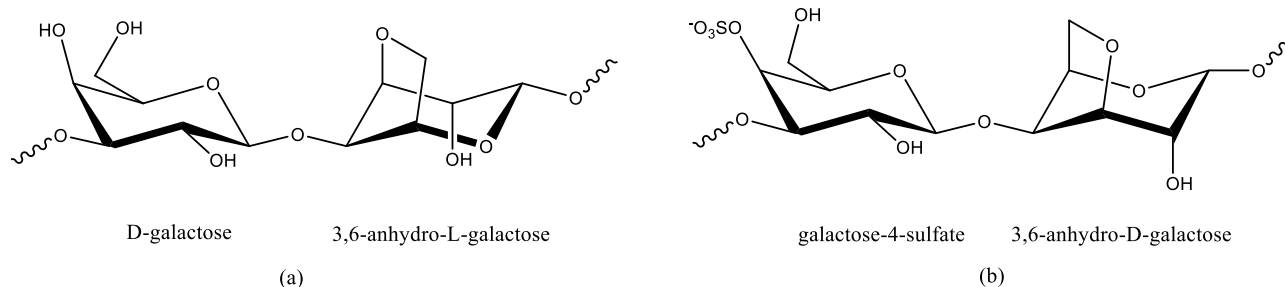


Figure 1. Molecular structures of agarose (a) and κ -carrageenan (b).

have favorable properties like a very fast growth rate, a high content of carbohydrates (up to 76% on dry weight),⁶ and limited amounts of lignin in the structure.⁴ Carrageenan and agar (consisting of agarose and agarpectin) are commercially used polysaccharides obtained from seaweed. The content of both biopolymers in red seaweed may be up to 88 and 42%, respectively.⁶ However, while the conversion of carrageenan as well as agarose (structures in Figure 1) for biobased chemicals has been studied in detail, far fewer efforts have been made on the conversion of 3,6-anhydro-galactose (AHG), the most abundant monomeric sugar of carrageenan and agarose, to HMF and LA (Table S1).

The synthesis of HMF and LA from κ -carrageenan and agarose using various homogeneous and heterogeneous catalysts in water and organic solvents has been reported (Table S2). The results are difficult to compare due to differences in reactor setups, substrate sources, and process conditions. The highest yield of HMF was reported to be 62 mol % in batch when using agarose and Amberlyst 36 as the catalyst and DMSO/water (7.2 wt % water) as the solvent at 140 °C and 180 min reaction time.⁷ Mondal *et al.* reported the highest yield of LA (82.4%) from an aqueous mixture enriched in galactose (GAL), which was obtained as a byproduct of HMF synthesis from κ -carrageenan.⁸

Of the two main building blocks in the polysaccharides in red seaweed (GAL and AHG, see Figure 1), GAL is known to be a poor source for HMF production, especially when using acid catalysts in water, leading to HMF yields <10 mol %.^{9,10} These findings indicate that AHG is most likely the precursor for HMF when using red seaweed or the individual biopolymers (κ -carrageenan and agarose) as the feed. This is in line with results from Kim *et al.*,¹¹ showing that agar (agarose and agarpectin) gave a 16 times higher HMF yield than GAL.

Our interest in the field is to obtain insights into the rates of the reactions of seaweed to HMF and LA. These kinetic models will be used as input for rational reactor design. To reduce complexity, we follow a systematic approach, starting with the individual monosaccharides (GAL, AHG), followed by conversions of the biopolymers (κ -carrageenan, agarose), and finally by using the actual seaweeds as the source. The focus of our research is on the use of water, a green and cheap solvent, and the use of mineral acids as the catalysts of choice. We here report a kinetic study on the conversion of 3,6-anhydro-D-galactose (D-AHG) to HMF and LA in water using sulfuric acid as the catalyst. To the best of our knowledge, such detailed studies have not been reported to date.

2. EXPERIMENTAL SECTION

2.1. Chemicals. 3,6-Anhydro-D-galactose (D-AHG, 95%) [CAS: 14122-18-0] was purchased from Dextra Laboratories. Sulfuric acid, H₂SO₄ (95–97 wt %) [7664-93-9] was purchased from Boom. HMF (99%) [67-47-0] and formic acid, FA ($\geq 95\%$) [64-18-6], were purchased from Sigma-Aldrich. LA (98%) [123-76-2] was purchased from Alfa Aesar. All chemicals were used without further purification. Milli-Q water was used to prepare the solutions.

2.2. Experimental Procedures. The experimental procedures are based on a procedure given by Girisuta *et al.*¹² The reactions were carried out in glass ampules with a length of 15 cm, internal diameter of 3 mm, and wall thickness of 1.5 mm. The glass ampules were filled with approximately 0.3 mL of the solution mixture consisting of D-AHG (0.006–0.06 M) and H₂SO₄ (0.0025–0.05 M). The ampules were then sealed with a torch. It is important to wear tinted safety goggles during the sealing procedure.

A series of ampules was placed in an aluminum rack and placed in a GC oven (Hewlett-Packard 5890A) set at a predetermined temperature (160–200 °C). Ampules were taken from the oven at certain times (0–480 min) and directly quenched in an ice-water bath to stop the reaction. For safety, quenching should always be carried out in a fume cupboard using proper gloves as occasionally an ampule breaks during quenching. The ampule was opened, and the reaction mixture was taken out. The mixture was filtered by using a 0.45 μ m PTFE filter to remove any insoluble materials. The composition of the clear solution was determined by using high-performance liquid chromatography (HPLC).

2.3. Analytical Methods. The composition of the reaction product was determined using an Agilent 1200 HPLC system equipped with an Agilent 1200 pump, an Aminex HPX-87H column, a refractive index detector, and an ultraviolet detector. The mobile phase was 5 mM sulfuric acid at a flow rate of 0.55 mL min⁻¹. The HPLC column was operated at 60 °C. The analysis of a sample was completed in 45 min. The concentrations of relevant components (a.o., D-AHG, HMF, LA) in the liquid phase were determined using calibration curves obtained by analyzing standard solutions of the individual components with known concentrations.

2.4. Definitions and Calculations. The concentrations of D-AHG, HMF, and LA were determined by using HPLC analysis. The conversion of D-AHG (X_{D-AHG}) and yield of HMF (Y_{HMF}) and LA (Y_{LA}) were calculated using eqs 1–3.

$$X_{D-AHG} \% = \frac{C_{D-AHG,0} - C_{D-AHG}}{C_{D-AHG,0}} \times 100 \quad (1)$$

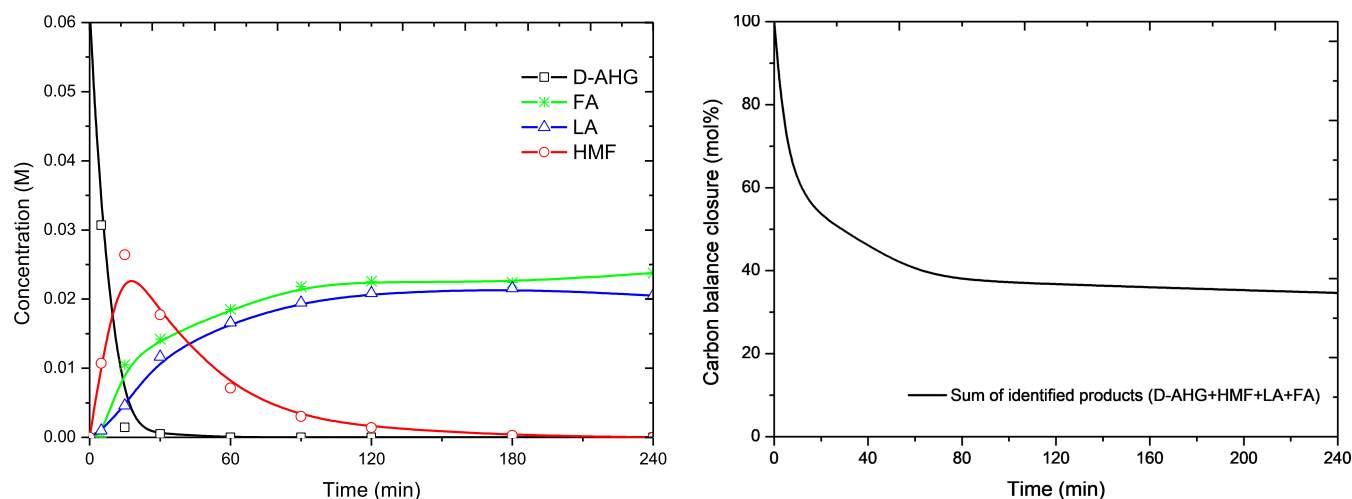


Figure 2. Concentration–time profile (left) and carbon balance (right) for a representative experiment (180 °C, $C_{D-AHG,0} = 0.06$ M, $C_{H_2SO_4} = 0.01$ M).

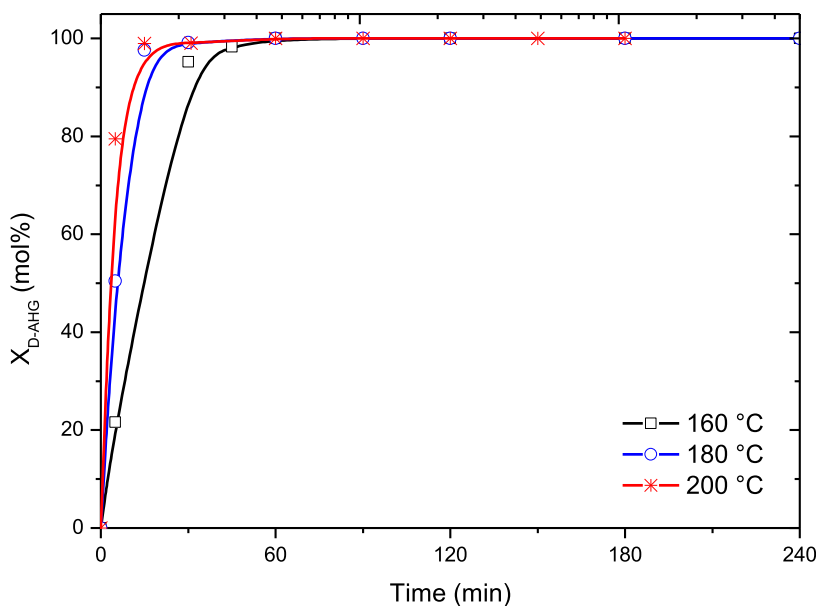


Figure 3. Conversion of D-AHG vs time at different temperatures. Conditions: $C_{AHG,0} = 0.06$ M and $C_{H_2SO_4} = 0.01$ M.

$$Y_{HMF} \% = \frac{C_{HMF} - C_{HMF,0}}{C_{D-AHG,0}} \times 100 \quad (2)$$

$$Y_{LA} \% = \frac{C_{LA} - C_{LA,0}}{C_{D-AHG,0}} \times 100 \quad (3)$$

The carbon balance was estimated based on the main HPLC detectable components (D-AHG, HMF, LA, and FA).

$$\begin{aligned} \% \text{ C balance} \\ = \frac{\text{C amount in products} + \text{C amount in remaining substrate}}{\text{C amount in starting substrate}} \times 100 \end{aligned} \quad (4)$$

3. RESULTS AND DISCUSSION

A total of 23 experimental series were performed in the temperature range of 160–200 °C with different initial concentrations of D-AHG ($C_{D-AHG,0}$, 0.006–0.06 M) and sulfuric acid ($C_{H_2SO_4}$, 0.0025–0.05 M). A representative

concentration versus time profile is shown in Figure 2 (left). As the reaction proceeds, the D-AHG concentration decreases and HMF, LA, and FA are formed. HMF shows a maximum value, indicating that it is an intermediate in the reaction network. Remarkably, GAL, an anticipated hydrolysis product of D-AHG, is not observed, and this gives information about the reaction network (*vide infra*). Besides these main components, small amounts of 1,2,4-benzenetriol (BTO) were formed as well (up to 10 mol %). BTO is a known reaction product from HMF when using water as the solvent.¹³

Besides these soluble products, brown/black insoluble compounds were formed, also known as humins. The amount of humins as a function of the batch time was estimated by performing carbon balance calculations for the main HPLC detectable components (D-AHG, HMF, LA, and FA), see Figure 2 (right) for details. The amount of humins increases over time and may be as high as 60 mol %, the exact amount depending on the reaction conditions. Isolated humin yields of up to 39 wt % have been reported for various sugars [glucose

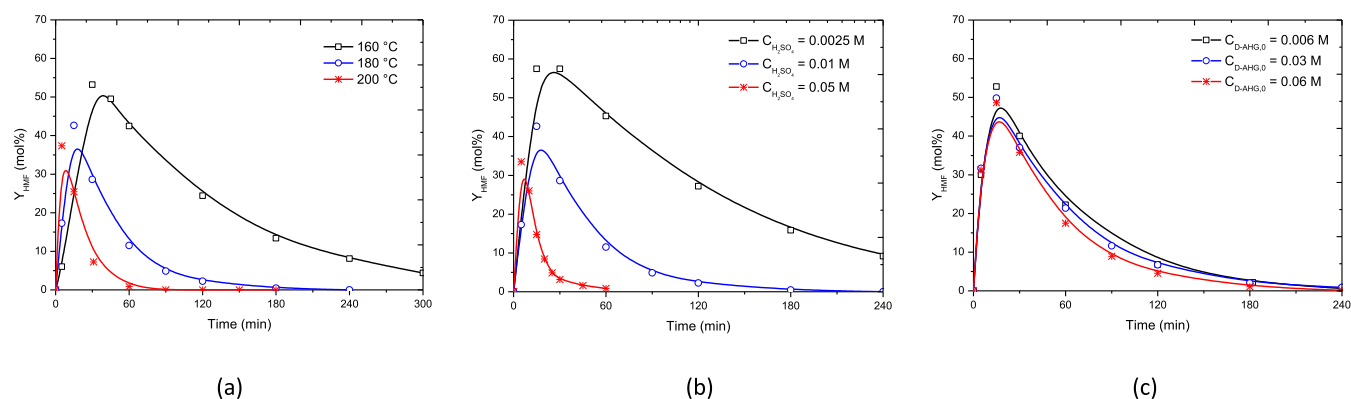


Figure 4. Yield of HMF versus time at (a) different temperatures ($C_{D-AHG,0} = 0.06$ M, $C_{H_2SO_4} = 0.01$ M), (b) different concentrations of H_2SO_4 (180 °C, $C_{D-AHG,0} = 0.06$ M), and (c) different initial concentrations of D-AHG (200 °C, $C_{H_2SO_4} = 0.0025$ M).

Table 1. Overview of Maximum HMF and LA for Hexoses in Water Using H_2SO_4 as the Catalyst

monosaccharide	temperature (°C)	$C_{sugar,0}$ (M)	$C_{H_2SO_4}$ (M)	max. Y_{HMF} (mol %)		max. Y_{LA} (mol %)		refs
				experiment	model	experiment	model	
GLU	140–200	0.1–1	0.05–1	<5 ^a	n.a.	60	n.a.	12
FRC	140–180	0.1–1	0.005–1	53 ^b	56	74	70	15
GAL	140–200	0.05–1	0.05–1	9 ^c	n.a.	51	54	10
D-AHG	160–200	0.006–0.06	0.0025–0.05	61 ^d	57	51	49	this work

^aReaction conditions are not available. ^bConditions: $T = 180$ °C, $C_{FRC,0} = 0.1$ M, $C_{H_2SO_4} = 0.01$ M. ^cConditions: $T = 200$ °C, $C_{GAL,0} = 0.055$ M, $C_{H_2SO_4} = 0.05$ M. ^dConditions: $T = 160$ °C, $C_{D-AHG,0} = 0.006$ M, $C_{H_2SO_4} = 0.0025$ M.

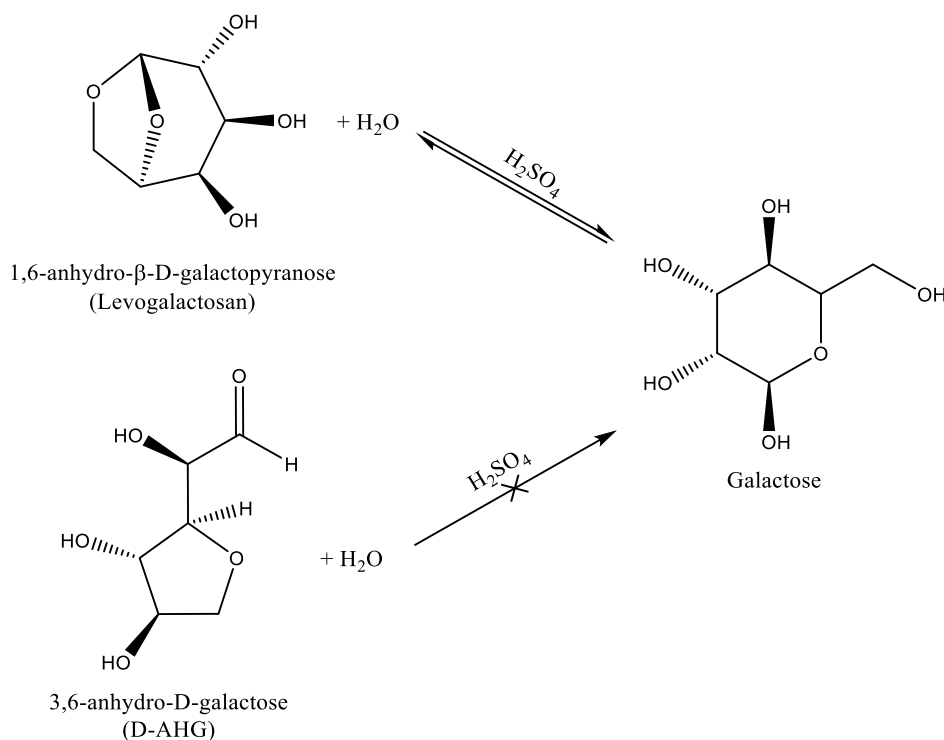


Figure 5. Comparison of reaction pathways for levogalactosan and D-AHG.

(GLU), fructose (FRC), xylose] in water at 180 °C with H_2SO_4 as the catalyst.¹⁴

The experimental reproducibility was tested by conducting several duplicate experiments. A representative result is given in the Supporting Information, Figure S1, and implies that the reproducibility of the experiments is good.

3.1. Effect of Process Variables on the Reactivity of D-AHG. The conversion of D-AHG is a strong function of temperature. Quantitative D-AHG conversion was obtained in less than 30 min at 200 °C, whereas it takes more than 60 min at 160 °C ($C_{D-AHG,0} = 0.06$ M, $C_{H_2SO_4} = 0.01$ M, Figure 3). The D-AHG conversion is independent of the initial D-AHG

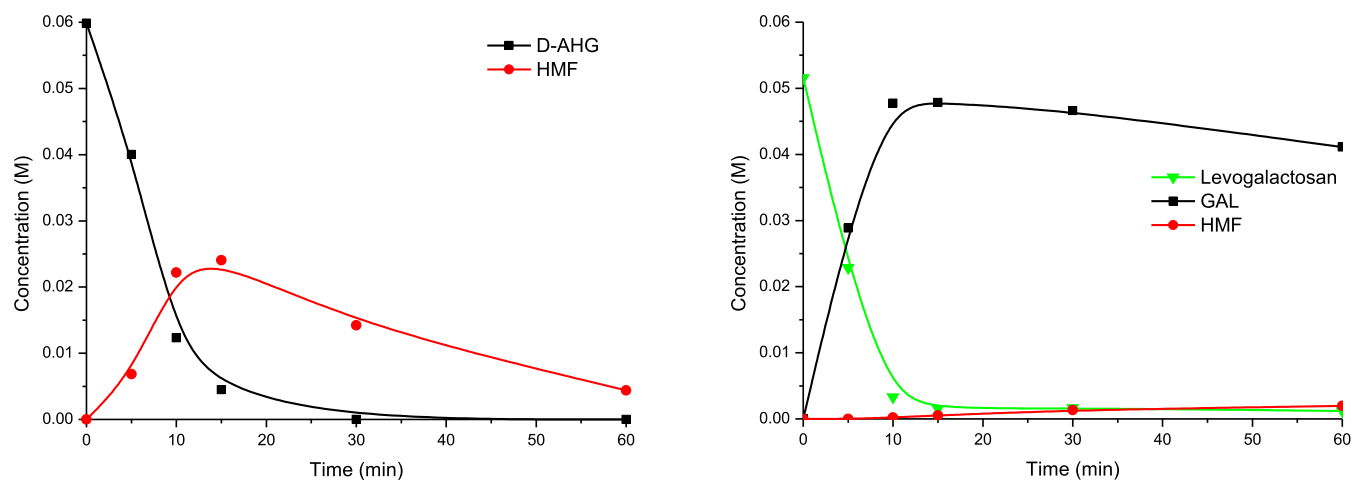
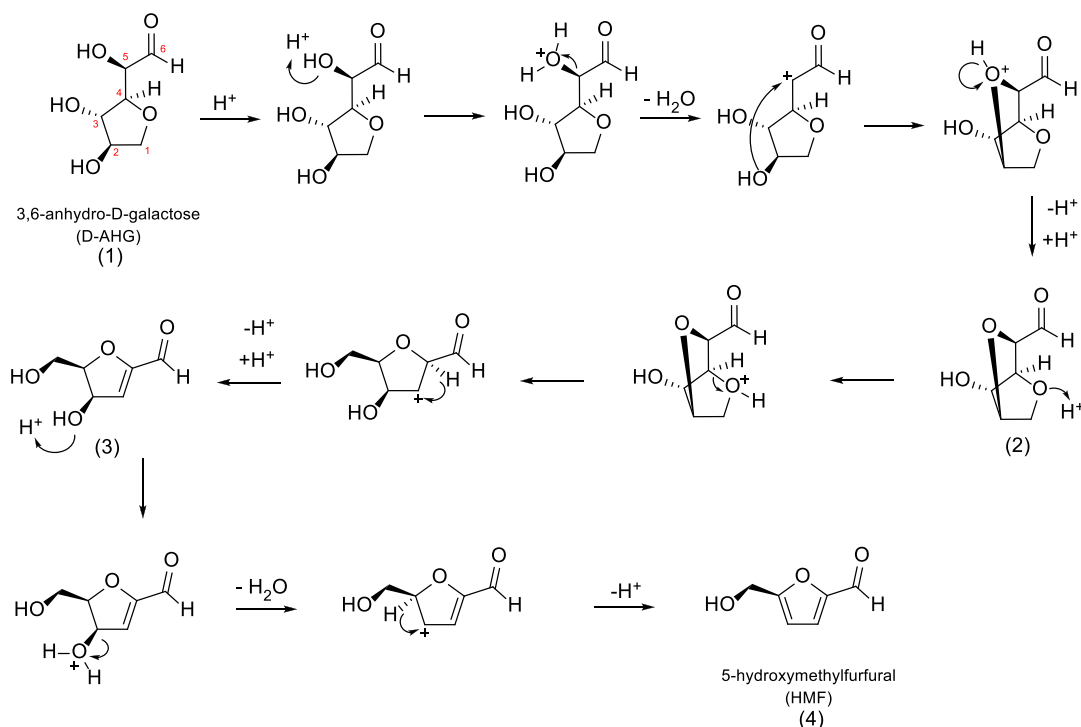


Figure 6. Comparison of the reactivities of D-AHG (left) and levogalactosan (right). Conditions: $C_{\text{H}_2\text{SO}_4} = 0.05 \text{ M}$; $T = 160 \text{ }^\circ\text{C}$.

Scheme 1. Proposed Reaction Mechanism for the Conversion of D-AHG to HMF



concentration (Figure S2, left), a strong indication that the reaction is first order in D-AHG. The sulfuric acid concentration has a major effect on the D-AHG conversion, and higher rates were observed at a higher sulfuric acid concentration (Figure S2, right).

3.2. Effect of Process Variables on the Yields of HMF. HMF is an intermediate product (Figure 2, left), formed from D-AHG and further reacting to LA and humins. As thus expected, the maximum HMF yield is a strong function of the process variables and particularly the batch time and to a lesser extent the temperature and acid concentration (Figure 4a,b). The highest experimental yield of HMF was 61 mol %, obtained at the lowest temperature in the range ($160 \text{ }^\circ\text{C}$). However, the initial D-AHG concentration only has a minor effect on the HMF yield (Figure 4c), indicating that the orders in reactants for the formation of HMF are about equal to those of the consecutive reactions to LA and humins. A kinetic

model (*vide infra*) was developed based on the experimental data and used to determine the conditions for the highest HMF yield within the experimental window of operation.

3.3. Comparison of HMF Yields with Other Sugars. To the best of our knowledge, studies that report HMF yields from pure D-AHG are not available to date. Compared with the reactivity of other hexoses in aqueous media using sulfuric acid as the catalyst in the same temperature range and batch setup (Table 1), the HMF yield from D-AHG (61 mol %) is higher than for fructose (FRC, 53 mol %), one of the best hexoses reported for HMF formation so far. The yields are also much higher than for the aldoses GAL (9 mol %) and GLU (5 mol %). As such, this anhydrosugar is a very special hexose for HMF synthesis and most likely also responsible for the good HMF yields when using carrageenan and seaweed as the feed.

Based on the high HMF yields from D-AHG compared to GAL, a reaction pathway involving an initial acid-catalyzed

hydrolysis of D-AHG to GAL followed by further reaction of GAL to HMF is highly unlikely, as the use of GAL as a feed leads to low HMF yields (Table 1). This is in marked contrast with the reactivity of another anhydrosugar derivative of galactose, *viz.* levogalactosan (1,6-anhydro- β -D-galactopyranose, Figure 5).

When levogalactosan is reacted with sulfuric acid in water at conditions in the range as used for D-AHG, the main product in the initial stage of the reaction is galactose, which is subsequently slowly converted to HMF (Figure 6). These findings imply that levogalactosan, a 1,6-anhydrosugar, is easily hydrolyzed to GAL, whereas this does not occur for D-AHG (3,6-anhydrosugar). In addition, it appears that D-AHG is much more reactive than GAL and levogalactosan. As such, another pathway from D-AHG to HMF is most likely taking place.

The proposed mechanism for the conversion of D-AHG to HMF is shown in Scheme 1. Here, the cyclic structures are given for clarity. It involves an initial dehydration of D-AHG (1) followed by acid-induced rearrangements to form a bicyclic structure (2). The latter was also proposed by Haworth *et al.*¹⁶ The bicyclic structure rearranges to (3), which then forms HMF (4).

Density functional theory calculations (Gaussian 16 package¹⁷) were performed to confirm the mechanistic proposal. The structures were optimized in the liquid phase (H₂O) at the B3LYP/311+(d,p) level. The Gibbs free energies (ΔG) were determined based on optimized structures, and the resulting energy profile for the formation of HMF from D-AHG is shown in Figure 7. All steps have a negative Gibbs free energy and thus seem thermodynamically feasible.

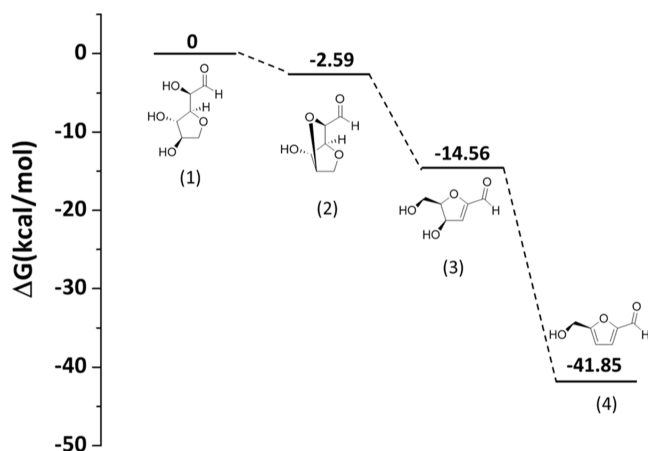


Figure 7. Modeled energy profile for the conversion of D-AHG to HMF.

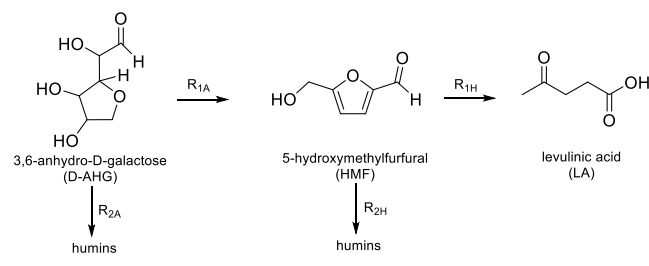
3.4. Effect of Process Variables on the Yields of LA.

The effect of process variables on the yield was also assessed for LA. Details and figures are given in the Supporting Information, Section S4. The highest experimentally observed LA yield was 51 mol %, similar to the yield when using GAL as the feed (Table 1) using the same experimental setup. This value is lower than that found for FRC (74 mol %) and GLU (60 mol %). As such, D-AHG seems to be a more appropriate feed for HMF than for LA formation.

3.5. Kinetic Modeling for the Acid-Catalyzed Hydrolysis of D-AHG to HMF and LA. A simplified reaction network for the sulfuric acid-catalyzed hydrolysis of D-AHG to

LA based on the experimental concentration *versus* time profiles is given in Scheme 2 where HMF is considered an intermediate product.

Scheme 2. Simplified Reaction Network for Acid-Catalyzed Hydrolysis of D-AHG to HMF and LA



The reaction rates were defined using a power-law approach; see eqs 5–8.

$$R_{1A} = k_{1A}(C_{D-AHG})^{a_A} \quad (5)$$

$$R_{2A} = k_{2A}(C_{D-AHG})^{b_A} \quad (6)$$

$$R_{1H} = k_{1H}(C_{HMF})^{a_H} \quad (7)$$

$$R_{2H} = k_{2H}(C_{HMF})^{b_H} \quad (8)$$

The temperature dependence of the kinetic constants was introduced by using modified Arrhenius equations (eqs 9–12).

$$k_{1A} = (C_{H^+})^{a_A} k_{1RA} \exp\left[\frac{E_{1A}}{R} \left(\frac{T-T_R}{T_R T}\right)\right] \quad (9)$$

$$k_{2A} = (C_{H^+})^{b_A} k_{2RA} \exp\left[\frac{E_{2A}}{R} \left(\frac{T-T_R}{T_R T}\right)\right] \quad (10)$$

$$k_{1H} = (C_{H^+})^{a_H} k_{1RH} \exp\left[\frac{E_{1H}}{R} \left(\frac{T-T_R}{T_R T}\right)\right] \quad (11)$$

$$k_{2H} = (C_{H^+})^{b_H} k_{2RH} \exp\left[\frac{E_{2H}}{R} \left(\frac{T-T_R}{T_R T}\right)\right] \quad (12)$$

T is a function of the batch time (see eq S3) and T_R is the reference temperature (140 °C). The concentration of H⁺ in aqueous solutions of sulfuric acid at different concentrations was calculated using eq 13.

$$C_{H^+} = C_{H_2SO_4} + \frac{1}{2} \left(- (K_{a,HSO_4^-}) + \sqrt{(K_{a,HSO_4^-})^2 + 4(C_{H_2SO_4} K_{a,HSO_4^-})} \right) \quad (13)$$

K_{a,HSO_4^-} in eq 13 represents the dissociation constant of HSO₄⁻ for which a value of 10^{-3.6} was applied.^{12,15} The concentrations of D-AHG, HMF, and LA as a function of time in a batch system are presented by differential equations given in eqs 14–16.

$$\frac{dC_{D-AHG}}{dt} = - (R_{1A} + R_{2A}) \quad (14)$$

$$\frac{dC_{HMF}}{dt} = R_{1A} - (R_{1H} + R_{2H}) \quad (15)$$

$$\frac{dC_{LA}}{dt} = R_{1H} \quad (16)$$

Table 2. Comparison of Several Kinetic Models of D-AHG Conversion to HMF and LA

parameter	value				
	model 1 ^a (original)	model 2 ^b	model 3 ^c	model 4 ^a	model 5 ^a
k_{1RA} ($M^{1-a_A-\alpha_A} \text{ min}^{-1}$)	0.056 ± 0.008	0.076 ± 0.011	0.062 ± 0.018	0.028 ± 0.006	0.079 ± 0.009
k_{2RA} ($M^{1-b_A-\beta_A} \text{ min}^{-1}$)	0.077 ± 0.018	0.031 ± 0.009	0.035 ± 0.012	0.027 ± 0.008	0.062 ± 0.011
E_{1A} (kJ mol ⁻¹)	68.9 ± 3.1	66.8 ± 6.5	60.5 ± 6.0	60.5 ± 4.7	69.1 ± 3.3
E_{2A} (kJ mol ⁻¹)	83.8 ± 5.1	87.8 ± 7.7	88.1 ± 7.0	71.8 ± 7.5	81.5 ± 5.4
a_A	0.92 ± 0.02	0.92 ± 0.03	0.96 ± 0.05	0.96 ± 0.04	1
b_A	1.04 ± 0.04	1.00 ± 0.05	0.95 ± 0.06	1.07 ± 0.06	1
α_A	0.26 ± 0.02	0.35 ± 0.04	0.24 ± 0.04	0	0.26 ± 0.02
β_A	0.37 ± 0.04	0.18 ± 0.05	0.26 ± 0.05	0	0.36 ± 0.04
k_{1RH} ($M^{1-a_H-\alpha_H} \text{ min}^{-1}$)	0.362 ± 0.066	0.176 ± 0.042	0.340 ± 0.010	0.366 ± 0.100	0.365 ± 0.043
k_{2RH} ($M^{1-b_H-\beta_H} \text{ min}^{-1}$)	0.005 ± 0.003	0.039 ± 0.017	0.117 ± 0.008	0.006 ± 0.006	0.008 ± 0.004
E_{1H} (kJ mol ⁻¹)	84.1 ± 2.9	79.5 ± 7.3	110.5 ± 0.7	84.3 ± 4.3	84.0 ± 3.0
E_{2H} (kJ mol ⁻¹)	95.3 ± 8.3	119.0 ± 9.8	111.0 ± 2.0	100.8 ± 14.2	99.7 ± 9.0
a_H	0.99 ± 0.03	1	0.88 ± 0.01	0.99 ± 0.04	1
b_H	0.90 ± 0.07	1	1.23 ± 0.03	0.90 ± 0.12	1
α_H	1.20 ± 0.02	0.90 ± 0.07	1.38 ± 0.02	1.21 ± 0.04	1.20 ± 0.03
β_H	0.53 ± 0.09	1.19 ± 0.10	1.07 ± 0.04	0.66 ± 0.08	0.56 ± 0.10
% FIT _{D-AHG}	93%	93%	93%	86%	93%
% FIT _{HMF}	81%	60%	61%	75%	81%
% FIT _{LA}	89%	63%	70%	88%	87%
AIC	-517	-400	-413	-450	-516

^aThis research. ^bKinetic parameter of HMF to LA and HMF to humins were taken from Martina *et al.*¹⁰ ^cKinetic parameter of HMF to LA and HMF to humins were taken from Girisuta *et al.*¹⁸

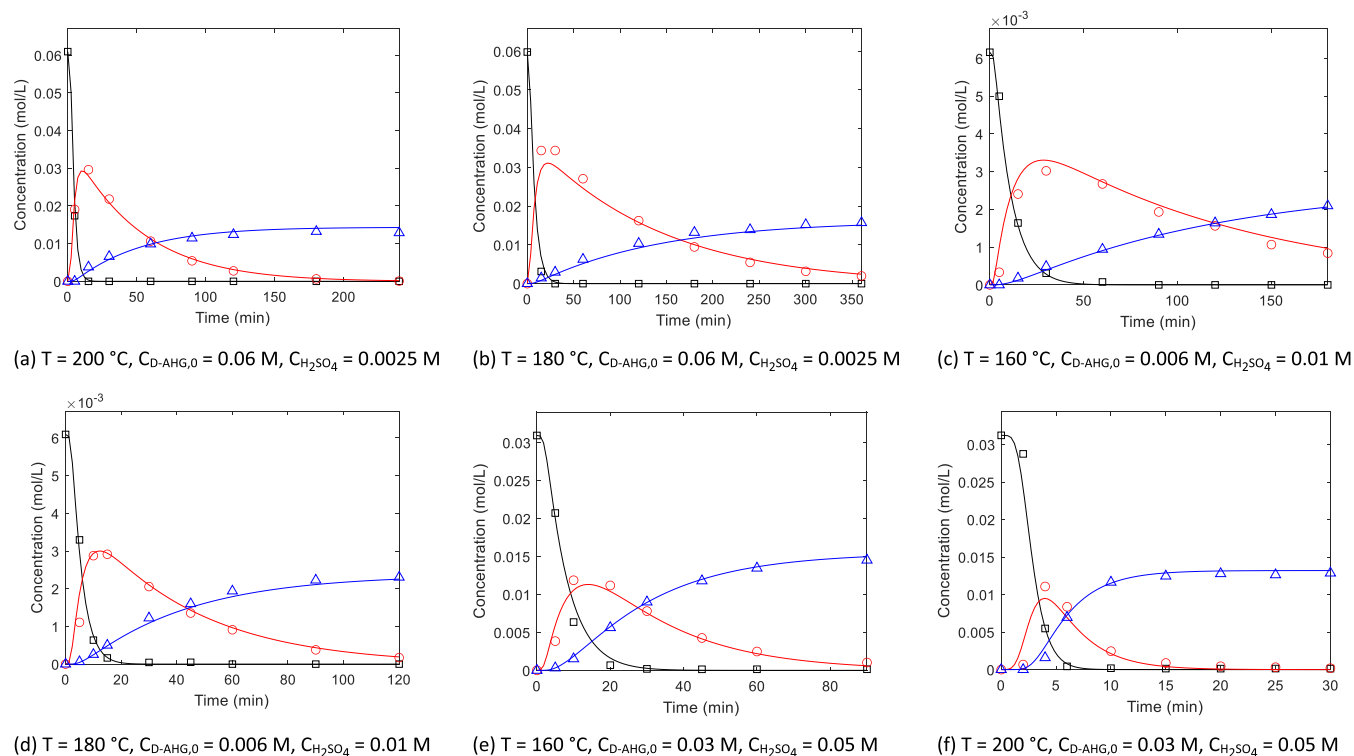


Figure 8. Comparison of the experimental data (black \square : D-AHG, red \circ : HMF, blue Δ : LA) and predicted data (solid lines) from the kinetic model.

A total of 612 data points (23 experiments, 8–9 samples per experiment, and concentrations of D-AHG, HMF, and LA for each sample) were used to develop the kinetic model. Kinetic parameters of the sulfuric acid-catalyzed hydrolysis of D-AHG were determined using a nonlinear regression method (lsqnonlin) in MATLAB R2020a. The best estimates of the

kinetic parameters for this model (model 1) are shown in Table 2. A comparison between the experimental data and the output of the kinetic model shows a good fit for a broad range of reaction conditions (Figure 8), as confirmed by a parity plot (Figure 9).

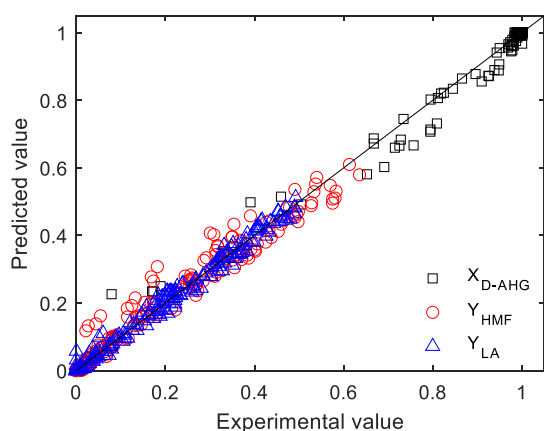


Figure 9. Parity plot of all experimental and predicted data points.

Several models with less parameters than model 1 have been tested (Table 2) and the goodness-of-fit approach¹⁸ and Akaike Information Criterion (AIC)¹⁹ were applied to compare the quality of the models (eqs 17–20). For the latter, the best model has the lowest value.

$$\% \text{FIT}_{\text{GAL}} = \left[1 - \frac{\text{norm}(C_{\text{GAL}} - \hat{C}_{\text{GAL}})}{\text{norm}(C_{\text{GAL}} - \bar{C}_{\text{GAL}})} \right] \times 100\% \quad (17)$$

$$\% \text{FIT}_{\text{HMF}} = \left[1 - \frac{\text{norm}(C_{\text{HMF}} - \hat{C}_{\text{HMF}})}{\text{norm}(C_{\text{HMF}} - \bar{C}_{\text{HMF}})} \right] \times 100\% \quad (18)$$

$$\% \text{FIT}_{\text{LA}} = \left[1 - \frac{\text{norm}(C_{\text{LA}} - \hat{C}_{\text{LA}})}{\text{norm}(C_{\text{LA}} - \bar{C}_{\text{LA}})} \right] \times 100\% \quad (19)$$

$$\text{AIC} = n \log \left(\frac{\sum \hat{\epsilon}_i^2}{2} \right) + 2k \quad (20)$$

In these equations, n is the number of data points, $\hat{\epsilon}_i$ is the estimated residuals from the fitted model, and k is the number of parameters in the model.

Model 2 is a model using the kinetic parameters for the conversion of HMF to LA obtained in previous research from our group using GAL as the feed,¹⁰ while model 3 uses the kinetic parameter obtained for the conversion of HMF to LA using HMF as the feed.¹⁸ By this approach, the number of model parameters reduces from 16 for model 1 to 8 for models 2 and 3. However, the goodness-of-fit, especially for the yields of HMF and LA, is reduced considerably.

Model 4 is a simplified version of model 1, where the order in sulfuric acid for the reaction D-AHG to HMF (α_A) and to humins (β_A) was set to 0. The rationale for this choice is the experimental observation that the acid concentration only gives a minor effect on the D-AHG conversion to HMF (Figure 4b). However, the model fit for particularly the HMF yield was poor, most likely because the yield of HMF is significantly affected by the acid concentration.

Model 5 is also a simplified version of model 1. In this case, the order of D-AHG to HMF (a_A) and humins (b_A), and further hydrolysis of HMF to LA (a_H) and humins (b_H), was set to 1 based on the observation that the optimized model parameters are 1 within the error limits. Confirmation that the order for D-AHG for the reaction of D-AHG to HMF is about 1 comes from the experiments using different initial concentrations of D-AHG, showing that the conversion of D-AHG is independent of the initial concentration (Figure S2, left). The % FIT and AIC values for this model are very similar to those of model 1. However, the number of parameters in model 5 (12) is lower than for model 1 (16) and was thus selected as the most appropriate model and will be used for the discussion in the next paragraphs.

3.6. Model Implications. Figure 10 shows the modeled yield of HMF as a function of the temperature and sulfuric acid catalyst concentration. In the temperature range used in this study (160–200 °C), the highest predicted yield of HMF (57 mol %) is achieved at temperature 160 °C and the lowest concentration of sulfuric acid (0.0025 M). The experimental HMF yield was 61 mol % at these conditions, indicating that the model represents the data very well. The highest predicted yield of LA (49 mol %, 160 °C, 0.05 M sulfuric acid, and 0.006

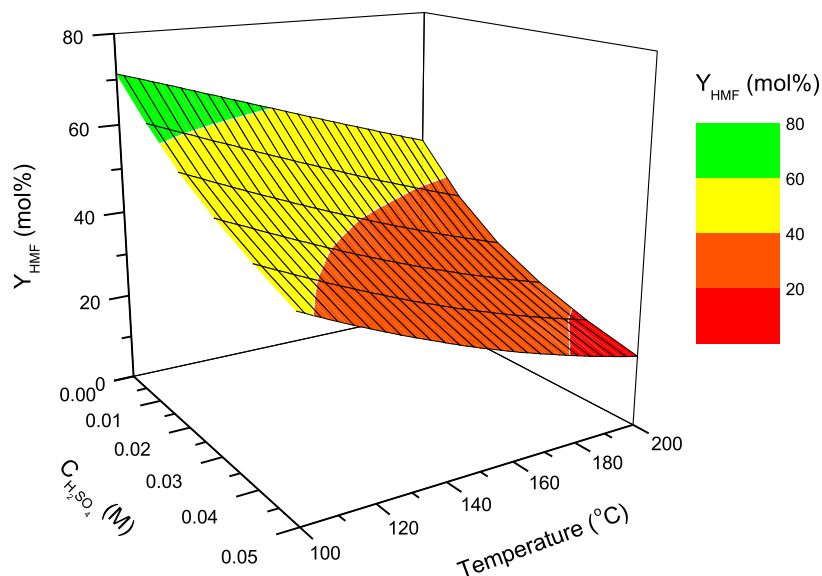


Figure 10. Effect of the temperature and sulfuric acid concentration on HMF yield. Conditions: $C_{\text{D-AHG},0} = 0.06$ M and $X_{\text{D-AHG}} = 100\%$.

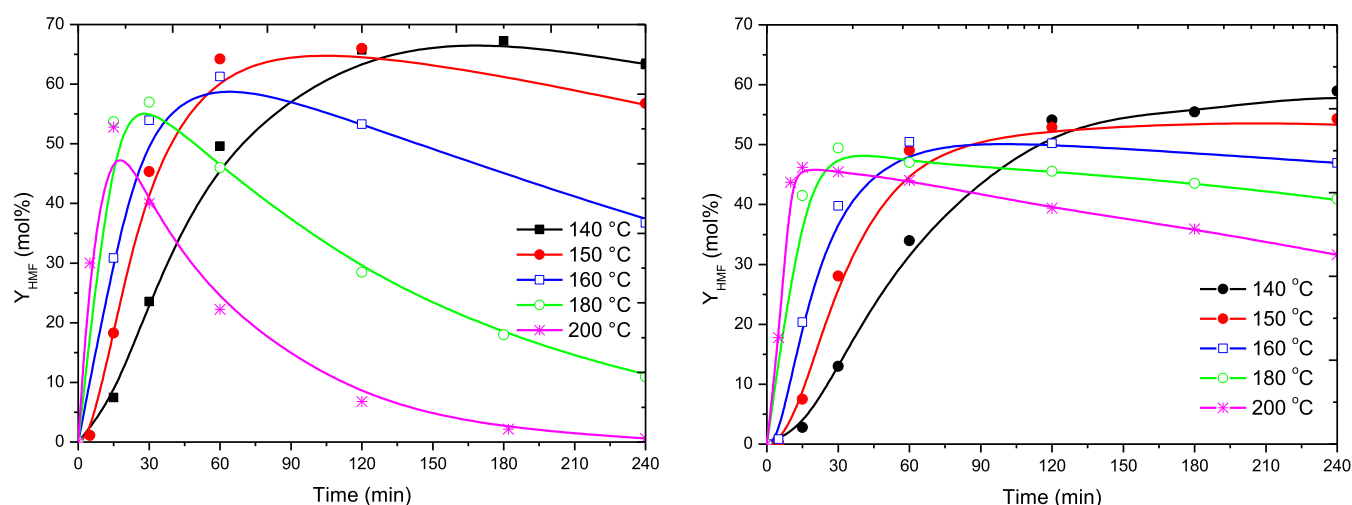


Figure 11. Experimental and modeled HMF yield versus time at different temperatures. Conditions: $C_{D-AHG,0} = 0.006$ M, $C_{H_2SO_4} = 0.0025$ M (left), and without H_2SO_4 (right).

M D-AHG) is also in good agreement with the experimental value of 51 mol % at these conditions (Table 1).

When considering the modeled HMF yields in Figure 10, it appears that the process conditions for the highest HMF yield are outside the experimental window. Actually, the highest yields are predicted at lower temperatures and lower acid concentrations (Figure 10). As such, some additional experiments were performed at lower temperatures and acid concentrations, and the results are shown in Figure 11. Indeed, the maximum yield of HMF tends to be higher at a lower temperature, either with (Figure 11, left) or without (Figure 11, right) the addition of H_2SO_4 . However, the effect is only limited when looking at the maximum yield at 160 °C (61 mol %), 150 °C (66 mol %), and 140 °C (67 mol %), while the reaction rates drop dramatically.

It also appears that the presence of acid is essential when considering HMF yields, and this is nicely illustrated in a comparison of the two graphs in Figure 11. The maximum HMF yields in the presence of sulfuric acid are 7–12 mol % higher than without a catalyst. However, it should be realized that lower temperatures and acid concentrations have a major effect on the reaction rate and thus also the volumetric production rate of HMF (mol HMF/ $m^3 \cdot h$). As such, further reactor optimization is required and the optimum conditions for the highest HMF productivity may not necessarily be in the lower temperature and acid range.

It was also proved possible to use the optimized model to predict the HMF yields outside the experimental temperature window (160–200 °C, Table 3). According to the model, the

Table 3. Comparison of the Experimental and Predicted Values of $Y_{HMF,max}$ at Different Temperatures^a

temperature	$Y_{HMF,max}$ (mol %)	
	experimental	predicted
140	67	62
150	66	59
160	61	57
180	57	57
200	53	47

^aConditions: $C_{D-AHG,0} = 0.006$ M, $C_{H_2SO_4} = 0.0025$ M.

highest HMF yield (62 mol %) is attainable at 140 °C, 0.0025 M sulfuric acid, and 0.006 M D-AHG. Additional experiments at this temperature confirmed the model, and the experimental value was 67 mol % at these conditions.

In addition, experiments were performed at a much higher initial D-AHG concentration (0.3 M, 5 wt %) than used in the original design (max 0.06 M, 1 wt %). The experimentally highest HMF yield is 62 mol % (Figure 12), whereas model 5

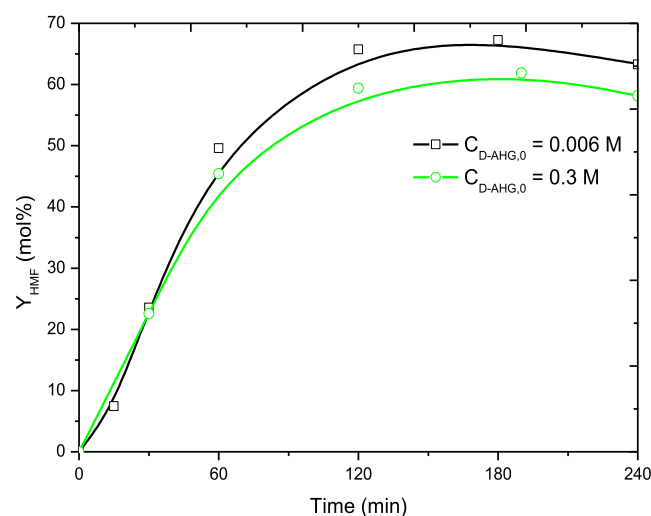


Figure 12. Experimental yield of HMF at various initial concentrations of D-AHG. $C_{H_2SO_4} = 0.0025$ M, and $T = 140$ °C.

predicts an HMF yield of 63 mol %. This shows that the model is also applicable at higher initial D-AHG concentrations. In addition, it shows that it is also possible to obtain high HMF yields at much higher initial D-AHG concentrations, which is highly beneficial from an industrial perspective.

It is of interest to compare the activation energies of the main reactions in the network from D-AHG to HMF and LA with those reported in the literature at similar conditions (sulfuric acid, water, temperature range between 80 and 200 °C). The results are listed in Figure 13. The activation energy for the conversion of D-AHG (69.1 ± 3.2 kJ mol⁻¹) to HMF is low compared to those of other hexoses. Values for the

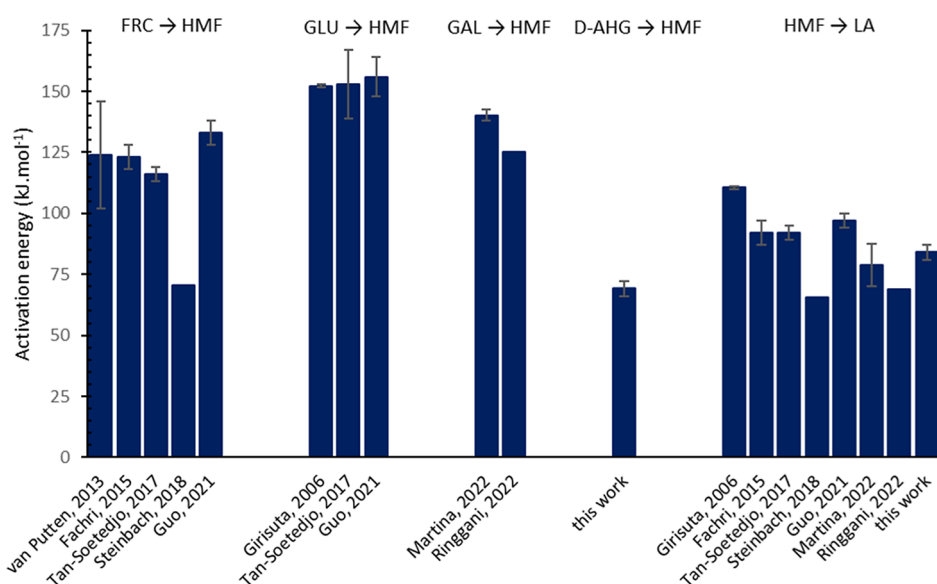


Figure 13. Activation energies for the conversion of sugars to HMF and HMF to LA in a sulfuric acid–water system.^{10,12,15,18,20–24}

activation energy for the conversion of hexoses to HMF are reported to be in the range 70.6–156 kJ mol⁻¹. Typical aldoses like GAL and GLU have higher activation energies (125–150 kJ mol⁻¹) than ketoses like FRC (<125 kJ mol⁻¹). The activation energy of the conversion of D-AHG to HMF is rather low (69.1 ± 3.2 kJ mol⁻¹) and among the lowest reported so far for hexoses. The activation energy for the reaction of HMF to LA found in this study (84.0 ± 3.0 kJ mol⁻¹) falls well within the ranges reported in the literature (65.4–110.5 kJ mol⁻¹).

3.6.1. Batch Simulation and Optimization. Kinetic model 5 was used to simulate the batch time for 90% D-AHG conversion and the selectivity of HMF and LA formation as a function of the process conditions. A plot for the batch time to reach 90% conversion *versus* the temperature is given in Figure 14 (red line) and ranges from 35 min at 160 °C to 5 min only at 200 °C. It is of interest to compare these batch times with those of other hexoses. For this purpose, kinetic input from

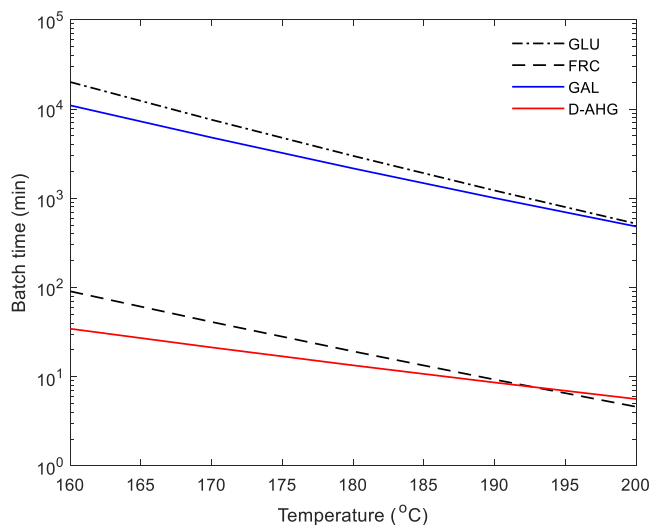


Figure 14. Required batch time for 90 mol % of monosaccharide (D-AHG, GAL, GLU, FRC) conversion as a function of temperature. Conditions: $C_{\text{sugar},0} = 0.006$ M; $C_{\text{H}_2\text{SO}_4} = 0.0025$ M.

previous studies from our group was used, also obtained in water, with sulfuric acid and the same experimental setup and analysis techniques. The result is given in Figure 14 and shows that D-AHG is by far more reactive than the aldoses GLU and GAL, whereas it is more reactive than FRC at low temperatures and slightly less reactive at temperatures above 190 °C.

The kinetic model also allows the prediction of the optimum reaction conditions to achieve the highest selectivity of HMF or LA. Details are given in the Supporting Information, Section S7.

3.6.2. Optimization of HMF Yield in Continuous Reactor Systems. Finally, we also performed simulations to obtain the highest HMF yields in continuous reactors. For this purpose, the two extremes with respect to mixing were compared, *viz.*, a continuously ideally stirred tank reactor CISTR and a plug flow reactor (PFR). The yield and selectivity of HMF in the PFR were determined using similar equations as given for the batch reactor using the residence time instead of the batch time (eqs 2 and S8), while eqs 21–25 were used to model the CISTR.

$$Y_{\text{HMF}} = \frac{C_{\text{HMF}}^{\text{out}} - C_{\text{HMF}}^{\text{in}}}{C_{\text{D-AHG}}^{\text{in}}} \quad (21)$$

$$\tau_{\text{CISTR}} = \frac{C_i^{\text{out}} - C_i^{\text{in}}}{R_i} \quad (22)$$

The relation between the D-AHG conversion ($X_{\text{D-AHG}}$) and τ_{CISTR} is given in eq 23.

$$\tau_{\text{CISTR}} = \frac{X_{\text{D-AHG}} C_{\text{D-AHG}}^{\text{in}}}{R_{1A} + R_{2A}} \quad (23)$$

Substituting eq 23 into eq 22 and executing some rearrangement give eqs 24 and 25.

$$C_{\text{HMF}}^{\text{out}} = \left(\frac{R_{1A} - R_{1H} - R_{2H}}{R_{1A} + R_{2A}} \right) C_{\text{D-AHG}}^{\text{in}} X_{\text{D-AHG}} \quad (24)$$

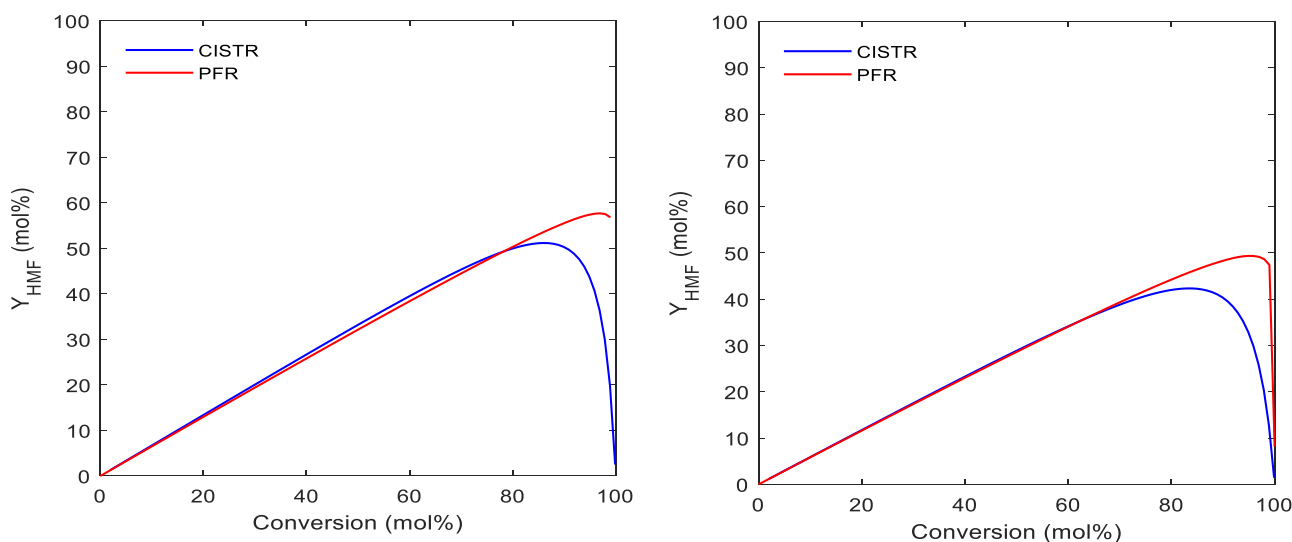


Figure 15. Comparison of the modeled HMF yield in CISTR and PFR at 160 °C (left) and 200 °C (right). Conditions: $C_{D-AHG,0} = 0.006$ M; $C_{H_2SO_4} = 0.0025$ M.

$$C_{LA}^{out} = \left(\frac{R_{1H}}{R_{1A} + R_{2A}} \right) C_{D-AHG}^{in} X_{D-AHG} \quad (25)$$

The yields of HMF as a function of D-AHG conversion at temperatures between 160 and 200 °C in the PFR and CISTR are provided in Figure 15, and those for LA are in the Supporting Information (Figure S8).

It is evident that the HMF yield is about equal in both the PFR and CISTR at D-AHG conversions lower than 70%. At higher conversions, PFR seems preferred. This result is in line with the reported study by Fachri *et al.* on HMF synthesis from FRC.¹⁵

3.7. Industrial Relevance of the Findings. The current study shows that D-AHG is an attractive precursor for HMF synthesis when considering HMF yields. To be a technoeconomically viable route, the HMF yield as such is not the only important criterion, and other factors should be considered as well. For instance, it is of relevance to use high initial D-AHG concentrations to (i) obtain high volumetric production rates (mol HMF/m³ reactor-h) to reduce the reactor size and (ii) minimize separation costs. The latter is a major issue for HMF production due to a.o. and its relatively low thermal stability. We have shown that indeed high HMF yields (62 mol %) are also attainable at industrially relevant high initial concentrations of D-AHG (5 wt %, Section 3.6) and as such, there are no limitations for using D-AHG as a source for HMF synthesis when considering this criterion.

To facilitate workup, liquid–liquid extraction using an organic solvent with a high affinity for HMF followed by further processing of this organic phase has shown to be very beneficial.² This extraction procedure may also be performed in the reactor by using a biphasic reaction system. This approach has shown to have a positive effect on HMF yields, while also facilitating the workup procedure to obtain pure HMF. Although this approach may also be implemented for the conversion of D-AHG to HMF, it has not been tested so far.

Finally, the techno-economic viability of bulk processes is highly dependent on the feedstock price. In contrast to FRC, a proven very suitable HMF source, D-AHG is not commercially available on a large scale. As such, it is pricewise currently

certainly not competitive with FRC. However, as stated in the introduction, D-AHG is a main building block of seaweeds and as such widely available. We are currently performing experimental studies using seaweed as the feed to obtain high HMF yields, among others, in biphasic systems. The best results so far are an HMF yield of 67 mol % at 152.5 °C, $C_{seaweed,0} = 1$ wt %, and $C_{HCl/AlCl_3} = 0.04$ M in a biphasic (water–MIBK) system, showing the potential of using a D-AHG rich feed for HMF synthesis. Details of this study will be reported in due course.

4. CONCLUSIONS

D-AHG, one of the major building blocks of macroalgae, is a promising feedstock for the synthesis of particularly HMF. The highest experimental HMF yields were up to 67 mol % and reveal that D-AHG is a by far better precursor for HMF synthesis than aldoses like GAL and GLU. The data also reveal that D-AHG is more reactive than FRC, GAL, and GLU. A molecular pathway is proposed for the formation of HMF from D-AHG involving a bicyclic intermediate. An initial D-AHG hydrolysis to GAL is not likely, as by far lower HMF yields are expected based on experiments with GAL only. The experimental data were successfully modeled by using a power law approach. The kinetic model was used to optimize the process conditions and the extent of back-mixing in continuous reactors. It showed that a PFR is favorable to achieve the highest yields of HMF. Additional experiments using higher initial concentrations of D-AHG (5 wt %) show that high HMF yields (62 mol %) are also possible at industrially relevant concentrations. Future work will involve the incorporation of the kinetic model obtained for D-AHG in kinetic models for the conversion of actual biopolymers (carrageenan and agarose) to HMF and ultimately as input for seaweed conversion models.

■ ASSOCIATED CONTENT

SI Supporting Information

The Supporting Information is available free of charge at <https://pubs.acs.org/doi/10.1021/acs.iecr.3c01357>.

AHG and GAL composition in seaweed polysaccharides, an overview of κ -carrageenan (κ C) and agarose conversion to platform chemicals, all experimental data series, D-AHG conversion to LA results, heat transfer experiments, data and model plot of all experimental series using model 1, and model applications using model 5 (PDF)

AUTHOR INFORMATION

Corresponding Author

Hero J. Heeres – Department of Chemical Engineering (ENTEG), University of Groningen, Groningen 9747 AG, The Netherlands; orcid.org/0000-0002-1249-543X; Email: h.j.heeres@rug.nl

Authors

Angela Martina – Department of Chemical Engineering (ENTEG), University of Groningen, Groningen 9747 AG, The Netherlands; Department of Chemical Engineering, Parahyangan Catholic University, Bandung 40141, Indonesia

Gorjan Stojkov – Department of Chemical Engineering (ENTEG), University of Groningen, Groningen 9747 AG, The Netherlands

Henk H. van de Bovenkamp – Department of Chemical Engineering (ENTEG), University of Groningen, Groningen 9747 AG, The Netherlands

Ting Wang – Department of Chemical Engineering (ENTEG), University of Groningen, Groningen 9747 AG, The Netherlands

Peter J. Deuss – Department of Chemical Engineering (ENTEG), University of Groningen, Groningen 9747 AG, The Netherlands; orcid.org/0000-0002-2254-2500

Inge W. Noordergraaf – Department of Chemical Engineering (ENTEG), University of Groningen, Groningen 9747 AG, The Netherlands

Jozef G. M. Winkelman – Department of Chemical Engineering (ENTEG), University of Groningen, Groningen 9747 AG, The Netherlands; orcid.org/0000-0001-7888-1731

Francesco Picchioni – Department of Chemical Engineering (ENTEG), University of Groningen, Groningen 9747 AG, The Netherlands; orcid.org/0000-0002-8232-2083

Complete contact information is available at:

<https://pubs.acs.org/10.1021/acs.iecr.3c01357>

Notes

The authors declare no competing financial interest.

ACKNOWLEDGMENTS

A.M. would like to thank the Directorate General of Higher Education, Ministry of Education, Culture, Research, and Technology, Indonesia (DIKTI), for providing her with a Ph.D. scholarship. T.M. acknowledges the China Scholarship Council for funding her PhD program (grant number 202006310031). The authors also thank Léon Rohrbach and Gert-Jan Boer for analytical support and Maarten Vervoort, Aad van der Weel, Erwin Wilbers, and Marcel de Vries for technical support.

NOMENCLATURE

α_A , reaction order of C_{D-AHG} in the decomposition of D-AHG to HMF (–)

α_A , reaction order of C_{H^+} in the decomposition of D-AHG to HMF (–)

α_H , reaction order of C_{HMF} in the decomposition of HMF to LA and FA (–)

α_H , reaction order of C_{H^+} in the decomposition of HMF to LA and FA (–)

b_A , reaction order of C_{D-AHG} in the decomposition of D-AHG to humins (–)

β_A , reaction order of C_{H^+} in the decomposition of D-AHG to humins (–)

b_H , reaction order of C_{HMF} in the decomposition of HMF to humins (–)

β_H , reaction order of C_{H^+} in the decomposition of HMF to humins (–)

C_{D-AHG} , concentration of D-AHG (M)

$C_{D-AHG,0}$, initial concentration of D-AHG (M)

C_{H^+} , concentration of H^+ (M)

$C_{H_2SO_4}$, concentration of sulfuric acid (M)

C_{HMF} , concentration of HMF (M)

$C_{HMF,0}$, initial concentration of HMF (M)

C_i^{in} , concentration of the i th compound at the inflow (M)

C_i^{out} , concentration of the i th compound at the outflow (M)

C_{LA} , concentration of LA (M)

$C_{LA,0}$, initial concentration of LA (M)

E_{1A} , activation energy of k_{1A} (kJ mol⁻¹)

E_{1H} , activation energy of k_{1H} (kJ mol⁻¹)

E_{2A} , activation energy of k_{2A} (kJ mol⁻¹)

E_{2H} , activation energy of k_{2H} (kJ mol⁻¹)

k_{1A} , reaction rate constant of D-AHG decomposition of HMF (M^{1- α_A} min⁻¹)

k_{1RA} , reaction rate constant k_{1A} at reference temperature (M^{1- α_A - α_A} min⁻¹)

k_{1H} , reaction rate constant of HMF for the main reaction (M^{1- α_H} min⁻¹)

k_{1RH} , reaction rate constant k_{1H} at reference temperature (M^{1- α_H - α_H} min⁻¹)

k_{2A} , reaction rate constant of D-AHG decomposition of humins (M^{1- β_A} min⁻¹)

k_{2RA} , reaction rate constant k_{2A} at reference temperature (M^{1- β_A - β_A} min⁻¹)

k_{2H} , reaction rate constant of HMF for the side reaction to humins (M^{1- β_H} min⁻¹)

k_{2RH} , reaction rate constant k_{2H} at reference temperature (M^{1- β_H - β_H} min⁻¹)

K_{a,H_2SO_4} , dissociation constant of (HSO₄)⁻ (–)

R , universal gas constant, 8.314 J mol⁻¹ K⁻¹

R_{1A} , reaction rate of D-AHG decomposition to HMF (mol L⁻¹ min⁻¹)

R_{1H} , reaction rate of HMF decomposition to LA (mol L⁻¹ min⁻¹)

R_{2A} , reaction rate of D-AHG decomposition to humins (mol L⁻¹ min⁻¹)

R_{2H} , reaction rate of HMF decomposition to humins (mol L⁻¹ min⁻¹)

t , time (min)

T_R , reference temperature (°C)

X_{D-AHG} , conversion of D-AHG (mol %)

Y_{HMF} , yield of HMF (mol %)

Y_{LA} , yield of LA (mol %)

SPECIAL SYMBOLS

\hat{C}_i , estimated value of matrix C_i (i = HMF, LA)

\bar{C}_i , average value of matrix C_i (i = HMF, LA)

Norm(C), norm of matrix C
% FIT_{*i*}, fit percentage of the *i*th compound (*i* = HMF, LA)

■ GREEK SYMBOLS

σ_{HMF} , selectivity of HMF (mol %)
 σ_{LA} , selectivity of LA (mol %)
 τ_{CISTR} , residence time of CISTR (min)

■ REFERENCES

- (1) Bozell, J. J.; Petersen, G. R. Technology Development for the Production of Biobased Products from Biorefinery Carbohydrates—the US Department of Energy's "Top 10" Revisited. *Green Chem.* **2010**, *12* (4), 539–555.
- (2) Van Putten, R. J.; Van Der Waal, J. C.; De Jong, E.; Rasrendra, C. B.; Heeres, H. J.; De Vries, J. G. Hydroxymethylfurfural, a Versatile Platform Chemical Made from Renewable Resources. *Chem. Rev.* **2013**, *113* (3), 1499–1597.
- (3) Hayes, G. C.; Becer, C. R. Levulinic Acid: A Sustainable Platform Chemical for Novel Polymer Architectures. *Polym. Chem.* **2020**, *11* (25), 4068–4077.
- (4) Signoretto, M.; Taghavi, S.; Ghedini, E.; Menegazzo, F. Catalytic Production of Levulinic Acid (LA) from Actual Biomass. *Molecules* **2019**, *24* (15), 2760.
- (5) Meinita, M. D. N.; Amron, A.; Trianto, A.; Harwanto, D.; Caesarendra, W.; Jeong, G. T.; Choi, J. S. Levulinic Acid Production from Macroalgae: Production and Promising Potential in Industry. *Sustainability* **2021**, *13* (24), 13919.
- (6) Holdt, S. L.; Kraan, S. Bioactive Compounds in Seaweed: Functional Food Applications and Legislation. *J. Appl. Phycol.* **2011**, *23* (3), 543–597.
- (7) Oh, S. J.; Park, J.; Na, J. G.; Oh, Y. K.; Chang, Y. K. Production of 5-Hydroxymethylfurfural from Agarose by Using a Solid Acid Catalyst in Dimethyl Sulfoxide. *RSC Adv.* **2015**, *5* (59), 47983–47989.
- (8) Mondal, D.; Sharma, M.; Maiti, P.; Prasad, K.; Meena, R.; Siddhanta, A. K.; Bhatt, P.; Ijardar, S.; Mohandas, V. P.; Ghosh, A.; Eswaran, K.; Shah, B. G.; Ghosh, P. K. Fuel Intermediates, Agricultural Nutrients and Pure Water from *Kappaphycus Alvarezii* Seaweed. *RSC Adv.* **2013**, *3* (39), 17989–17997.
- (9) Flannelly, T.; Lopes, M.; Kupiainen, L.; Dooley, S.; Leahy, J. J. Non-Stoichiometric Formation of Formic and Levulinic Acids from the Hydrolysis of Biomass Derived Hexose Carbohydrates. *RSC Adv.* **2016**, *6* (7), 5797–5804.
- (10) Martina, A.; Van De Bovenkamp, H. H.; Noordergraaf, I. W.; Winkelman, J. G. M.; Picchioni, F.; Heeres, H. J. Kinetic Study on the Sulfuric Acid-Catalyzed Conversion of d -Galactose to Levulinic Acid in Water. *Ind. Eng. Chem. Res.* **2022**, *61* (26), 9178–9191.
- (11) Kim, B.; Jeong, J.; Shin, S.; Lee, D.; Kim, S.; Yoon, H. J.; Cho, J. K. Facile Single-Step Conversion of Macroalgal Polymeric Carbohydrates into Biofuels. *ChemSusChem* **2010**, *3* (11), 1273–1275.
- (12) Girisuta, B.; Janssen, L. P. B. M.; Heeres, H. J. Green Chemicals: A Kinetic Study on the Conversion of Glucose to Levulinic Acid. *Chem. Eng. Res. Des.* **2006**, *84* (5), 339–349.
- (13) Kumalaputri, A. J.; Randolph, C.; Otten, E.; Heeres, H. J.; Deuss, P. J. Lewis Acid Catalyzed Conversion of 5-Hydroxymethylfurfural to 1,2,4-Benzenetriol, an Overlooked Biobased Compound. *ACS Sustain. Chem. Eng.* **2018**, *6* (3), 3419–3425.
- (14) van Zandvoort, I.; Wang, Y.; Rasrendra, C. B.; van Eck, E. R. H.; Buijninx, P. C. A.; Heeres, H. J.; Weckhuysen, B. M. Formation, Molecular Structure, and Morphology of Humins in Biomass Conversion: Influence of Feedstock and Processing Conditions. *ChemSusChem* **2013**, *6* (9), 1745–1758.
- (15) Fachri, B. A.; Abdilla, R. M.; Bovenkamp, H. H. V. D.; Rasrendra, C. B.; Heeres, H. J. Experimental and Kinetic Modeling Studies on the Sulfuric Acid Catalyzed Conversion of d -Fructose to 5-Hydroxymethylfurfural and Levulinic Acid in Water. *ACS Sustain. Chem. Eng.* **2015**, *3* (12), 3024–3034.
- (16) Haworth, W. N.; Jackson, J.; Smith, F. The Properties of 3: 6-Anhydrogalactose. *J. Chem. Soc.* **1940**, 620–632.
- (17) Frisch, M. J.; et al. *Gaussian 16*, Rev. B.01; Gaussian, Inc.: Wallingford CT, 2016.
- (18) Girisuta, B.; Janssen, L. P. B. M.; Heeres, H. J. A Kinetic Study on the Decomposition of 5-Hydroxymethylfurfural into Levulinic Acid. *Green Chem.* **2006**, *8* (8), 701–709.
- (19) Akaike, H. A New Look at the Statistical Model Identification. *IEEE Trans. Autom. Control* **1974**, *19* (6), 716–723.
- (20) van Putten, R. J.; Soetedjo, J. N. M.; Pidko, E. A.; Van Der Waal, J. C.; Hensen, E. J. M.; de Jong, E.; Heeres, H. J. Dehydration of Different Ketoses and Aldoses to 5-Hydroxymethylfurfural. *ChemSusChem* **2013**, *6* (9), 1681–1687.
- (21) Tan-Soetedjo, J. N. M.; Van De Bovenkamp, H. H.; Abdilla, R. M.; Rasrendra, C. B.; Van Ginkel, J.; Heeres, H. J. Experimental and Kinetic Modeling Studies on the Conversion of Sucrose to Levulinic Acid and 5-Hydroxymethylfurfural Using Sulfuric Acid in Water. *Ind. Eng. Chem. Res.* **2017**, *56* (45), 13228–13239.
- (22) Steinbach, D.; Kruse, A.; Sauer, J.; Vetter, P. Sucrose Is a Promising Feedstock for the Synthesis of the Platform Chemical Hydroxymethylfurfural. *Energies* **2018**, *11* (3), 645.
- (23) Guo, W.; Zhang, Z.; Hacking, J.; Heeres, H. J.; Yue, J. Selective Fructose Dehydration to 5-Hydroxymethylfurfural from a Fructose-Glucose Mixture over a Sulfuric Acid Catalyst in a Biphasic System: Experimental Study and Kinetic Modelling. *Chem. Eng. J.* **2021**, 409 (November 2020), 128182.
- (24) Ringgani, R.; Azis, M. M.; Rochmadi, R.; Budiman, A. Experimental and Kinetic Modeling of Galactose Valorization to Levulinic Acid. *Bull. Chem. React. Eng. Catal.* **2022**, *17* (2), 451–465.